Trans-Concerted Addition to Alkynes: the case of Ynamide Silylzincation

Frédéric Guégan, Fabrice Chemla, Franck Ferreira, Hélène Gérard, Alejandro Perez-Luna, Stéphanie Halbert

Chemistry–A European Journal

Research Article
doi.org/10.1002/chem.202401751

Chemistry Europe
European Chemical Societies Publishing

www.chemeurj.org

Trans-Concerted Addition to Alkynes: the case of Ynamide Silylzincation

Frédéric Guégan,[a, c] Fabrice Chemla,[b] Franck Ferreira,[b] Hélène Gérard,[a] Alejandro Perez-Luna,*[b] and Stéphanie Halbert*[a]

An original concerted antarafacial mechanism for the addition of diorganosilyl-zinc reagents across the C–C triple bond of ynamides is computationally investigated using DFT calculations. This concerted mechanism, leading to a *trans*-product in only one step, results in the formation of a Si–C and a Zn–C σ-bond on opposite sides of the π-system. We demonstrate that the mechanism going through a η^2-vinyl intermediate and the proposal of a radical chain pathway are energetically unsustainable. The retained concerted antarafacial pathway is tested on experimental selectivities: the regioselectivity, in favor of the silyl β-addition in ynamide, and stereoselectivity, which is *cis*- with $(Me_2PhSi)_2Zn$ but *trans*- with $[(Me_3Si)_3Si]_2Zn$, are well reproduced by DFT calculations. The regio- and stereoselectivity are discussed using the activation strain model and a chemical bonding analysis.

Introduction

Alkyne silylmetalation, *i.e.* the 1,2-addition of silicon–metal bonds across the carbon–carbon triple bond of alkynes, represents a valuable method for the construction of multi-substituted alkenes, and considerable efforts have been devoted to develop procedures allowing for high levels of regio- and stereocontrol.[1] The majority of the reported alkyne silylmetalation reactions occur through the insertion of the carbon–carbon triple bond into a silicon–transition-metal bond.[2] The addition of Si–Zn bonds across terminal alkyl-, aryl-substituted alkynes was achieved from di[3]- or monoanion[4]-type zincates, as well as from silyl-zinc species generated in-situ from silylboranes.[5] Such addition processes are *cis*-stereoselective and lead (primarily) to silylmetalation products with the newly formed bonds in *cis* configuration.

Recently, as part of our efforts to develop silylzincation in the quest for the elusive *trans* stereoselectivity,[6] we uncovered a remarkable dichotomy in the reactivity of disilylzinc reagents. Indeed, both $(Me_2PhSi)_2Zn$ and $[(Me_3Si)_3Si]_2Zn$ achieve the β-regioselective silylzincation of ynamide in the absence of any transition metal (Scheme 1, middle), but the stereoselectivity varied with the silyl group: Me_2PhSi gave the *cis*- and $(Me_3Si)_3Si$

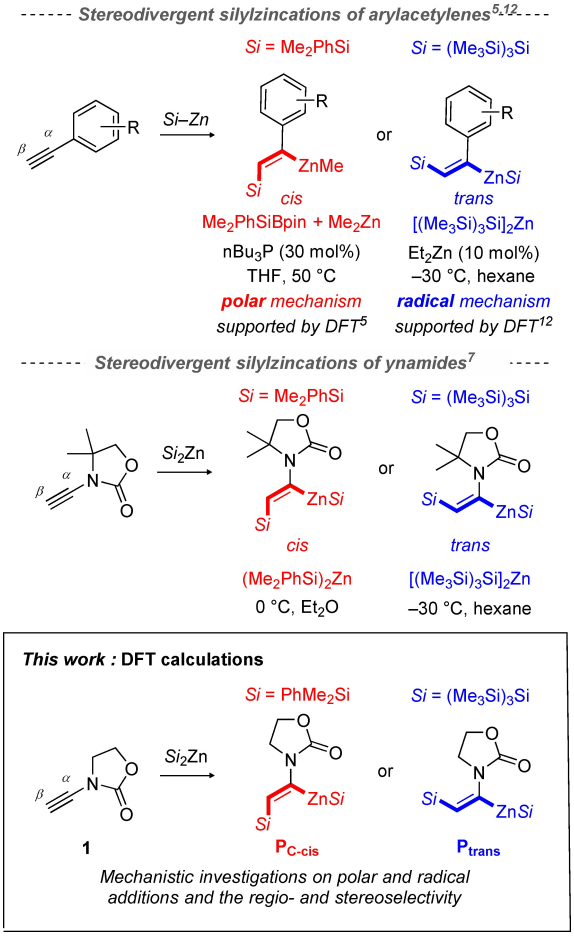

Scheme 1. State of art of the stereodivergent silylzincation of arylacetylenes and terminal ynamides with $(Me_2PhSi)_2Zn$ or $[(Me_3Si)_3Si]_2Zn$ reagents.

[a] *Dr. F. Guégan, H. Gérard, Dr. S. Halbert*
Sorbonne Université, CNRS, Laboratoire de Chimie Théorique, LCT
F–75005 Paris, France
E-mail: stephanie.halbert@sorbonne-universite.fr

[b] *F. Chemla, F. Ferreira, Dr. A. Perez-Luna*
Sorbonne Université, CNRS, Institut Parisien de Chimie Moléculaire, IPCM
F–75005 Paris, France
E-mail: alejandro.perez_luna@sorbonne-universite.fr

[c] *Dr. F. Guégan*
Present Address: Institut de Chimie des Milieux et matériaux de Poitiers, CNRS, Université de Poitiers,
1 rue Marcel Doré, 86073 Poitiers, France

Supporting information for this article is available on the WWW under https://doi.org/10.1002/chem.202401751

gave the *trans*-product.[7,8] Owing to the capacity of tris(trimethylsilyl)silyl to support radical chain mechanisms,[9] we ascribed the stereodivergent behavior to a competition between the established polar *cis*-addition pathway in the case of $(Me_2PhSi)_2Zn$ and a radical chain mechanism for $[(Me_3Si)_3Si]_2Zn$ analogous to oxygen initiated radical alkylzinc group-transfer processes.[10,11] A similar stereodivergent behaviour was also found in the case of terminal arylacetylenes (Scheme 1, top).[12] In this case, we found that $[(Me_3Si)_3Si]_2Zn$ reagent delivers the *trans*-silylzincation products, contrary to $(Me_2PhSi)ZnMe$ reagent which reacts with *cis* stereoselectivity through a polar addition mechanism (supported by DFT study).[5] In our report, experimental evidence for the radical behaviour of this reagent was provided and the theoretical mechanistic study on radical pathway supports the observed *trans*-stereoselectivity. Here, however, the silylzincation of aryl-substituted acetylenes only proceeded in the presence of added Et_2Zn, by contrast with the reaction of ynamides (Scheme 1, middle). Intrigued by this observation and given that Et_2Zn might serve as radical initiator, we decided to investigate computationally the mechanisms of addition of disilylzinc reagents across terminal ynamides (Scheme 1, bottom).

In the literature, only two examples described a combined experimental and computational study on the silylzincation of C–C multiple bonds (phenylallene or terminal alkyne) using $(PhMe_2Si)ZnR$ reagent (R=Me, tBu).[5,13] In these studies, the silylmetalation takes place directly from the two reactants through distorted transition state (TS), in which the silyl and zinc groups are in the same side of the C–C bond, corresponding to a *cis*-silylmetalation. In addition, several theoretical studies of *cis*-silylmetalation in hydrosilylation reactions have been extensively examined in transition-metal-catalysis (Pt, Rh, Co, Fe, Ir).[14,15,16] Different mechanisms were proposed, from the known Chalk-Harrod mechanism[15] to the modified one[16] and both imply the formation of a π-complex with the coordination of metal into the unsaturated bond. In the case of zinc(II) metal, the formation of alkene-zinc complexes is extremely rare as the π-back-bonding from a filled zinc d-orbital into the π^*-orbital of the olefin is weak due to the very high energy of zinc d orbitals.[17] For *trans*-silylmetalation, the *trans*-hydrosilylation products are generally believed to be derived from initial *cis*-silylmetalation followed by olefin isomerization.[18–20] In the case of cationic Ru-catalyzed hydrosilylation of terminal alkynes, it was proposed that the *trans*-addition stereochemistry results from the formation of metallocyclopropene intermediates.[21–22] More recently, this intermediate was proposed for the *trans*-selective carbosilylation of terminal alkyne with nickel catalyst.[23]

In this paper, we investigate the mechanism of silylzincation of ynamides using DFT calculations. For the $[(Me_3Si)_3Si]_2Zn$ reagent, the originally proposed radical pathway leading to the *trans*-isomer is first explored. For the *cis*-product, the traditional *cis*-silylmetalation, considered as polar mechanism, is next investigated. For the *trans*-product formation, we consider two pathways: an isomerization step from *cis*- to *trans*-product by analogy with the previous studies[21] and an alternative pathway leading in only one step to the *trans*-product. The most favorable pathway is discriminated on energetic aspects, in particular the activation barriers, and supported by the evaluation of selectivity. For this purpose, we test the most favorable mechanism for the regio- (α or β-additions) and stereoselectivity (relative to the silyl groups $[(Me_3Si)_3Si]_2Zn$ *vs.* $[(Me_2PhSi)]_2Zn$) and compare the computed selectivity with the experimental data. The stereo- and regioselectivity is finally discussed using the *activation strain* model and a chemical bonding analysis.

Results and Discussion

The radical silylzincation mechanism is first explored (Figure 1, geometric and energetic patterns are gathered in Table S1) using the following models (Scheme 1, bottom): ynamide **1** and $[(Me_3Si)_3Si]_2Zn$. The mechanism proposed is a chain mechanism involving the $Si(SiMe_3)_3$ radical, which is regenerated in the product formation step. The initiation step is not discussed here for reasons which will appear later. The first step of the radical propagation is the addition of the $(Me_3Si)_3Si$ radical across the C≡C triple bond in **1**, with an activation barrier calculated at 14.2 kcal mol^{-1}. The corresponding transition state $\mathbf{TS_{add}}$ is early, indicated by the large Si–C_β distance of 2.82 Å (*vs.* 1.92 Å in the formed Si–C_β bond in $\mathbf{I_{rad\text{-}trans}}$), and the slightly bent geometry of the alkyne (N–C_α–C_β angle of 169° in $\mathbf{TS_{add}}$ *vs.* 177° in ynamide **1**). The resulting vinyl radical $\mathbf{I_{rad\text{-}trans}}$ featuring a *trans* bending at C_α (N–C_α–C_β of 138°) is stable with a relative Gibbs Energy of −7.1 kcal mol^{-1}. The isomerization from *trans*- ($\mathbf{I_{rad\text{-}trans}}$) to *cis*-vinyl radical ($\mathbf{I_{rad\text{-}cis}}$) is accessible through a transition state $\mathbf{TS_{rad\text{-}isom}}$ characterized by a linear N–C_α–C_β angle of 178°. This isomerization is reversible with a low activation barrier of 4.9 kcal mol^{-1} between $\mathbf{I_{rad\text{-}trans}}$ and $\mathbf{TS_{rad\text{-}isom}}$ and slightly in favor of *cis* vinyl radical $\mathbf{I_{rad\text{-}cis}}$ (more stable by only 4 kcal mol^{-1} over $\mathbf{I_{rad\text{-}trans}}$). The electron in $\mathbf{I_{rad\text{-}cis}}$ and $\mathbf{I_{rad\text{-}trans}}$, stabilized by the nitrogen atom[24] of the oxazolidinone substituent, is localized on C_α as represented by the spin density in Figure S1.

The second step results from the reaction of *cis* or *trans* vinyl radical $\mathbf{I_{rad}}$ with $[(Me_3Si)_3Si]_2Zn$. As previously found for 2-ethynylanisole,[12] it also occurs in a single step with ynamide **1**. The coordination of $[(Me_3Si)_3Si]_2Zn$ to $\mathbf{I_{rad}}$ is associated with a cleavage of one of the Zn–Si bonds leading to the regeneration of the $(Me_3Si)_3Si$ radical and the formation of the silylzincation products **P**. The formation of products $\mathbf{P_{cis}}$ and $\mathbf{P_{trans}}$ relative to the separated reactants, ynamide **1** and $(Me_3Si)_3Si$ radical, is highly exergonic (−29.8 and −32.8 kcal mol^{-1}, respectively). In addition, this homolytic substitution is the rate-determining step as the activation barrier is the highest of the mechanism. It is also stereoselective as the *trans*-product $\mathbf{P_{trans}}$ is kinetically and thermodynamically favored over the *cis*-product $\mathbf{P_{cis}}$ by 9.4 and 3 kcal mol^{-1}, respectively, in line with the experimental observations. The stereodivergence originates thus in the second step, namely the radical chain transfer at the Zn center.

The structures of the two stereodetermining transition states $\mathbf{TS_{rad\text{-}cis}}$ and $\mathbf{TS_{rad\text{-}trans}}$ are represented in Figure 2 (geometrical parameters are available in Table S1). The approach of $[(Me_3Si)_3Si]_2Zn$ to vinyl radical **I** is associated with large Zn–C_α

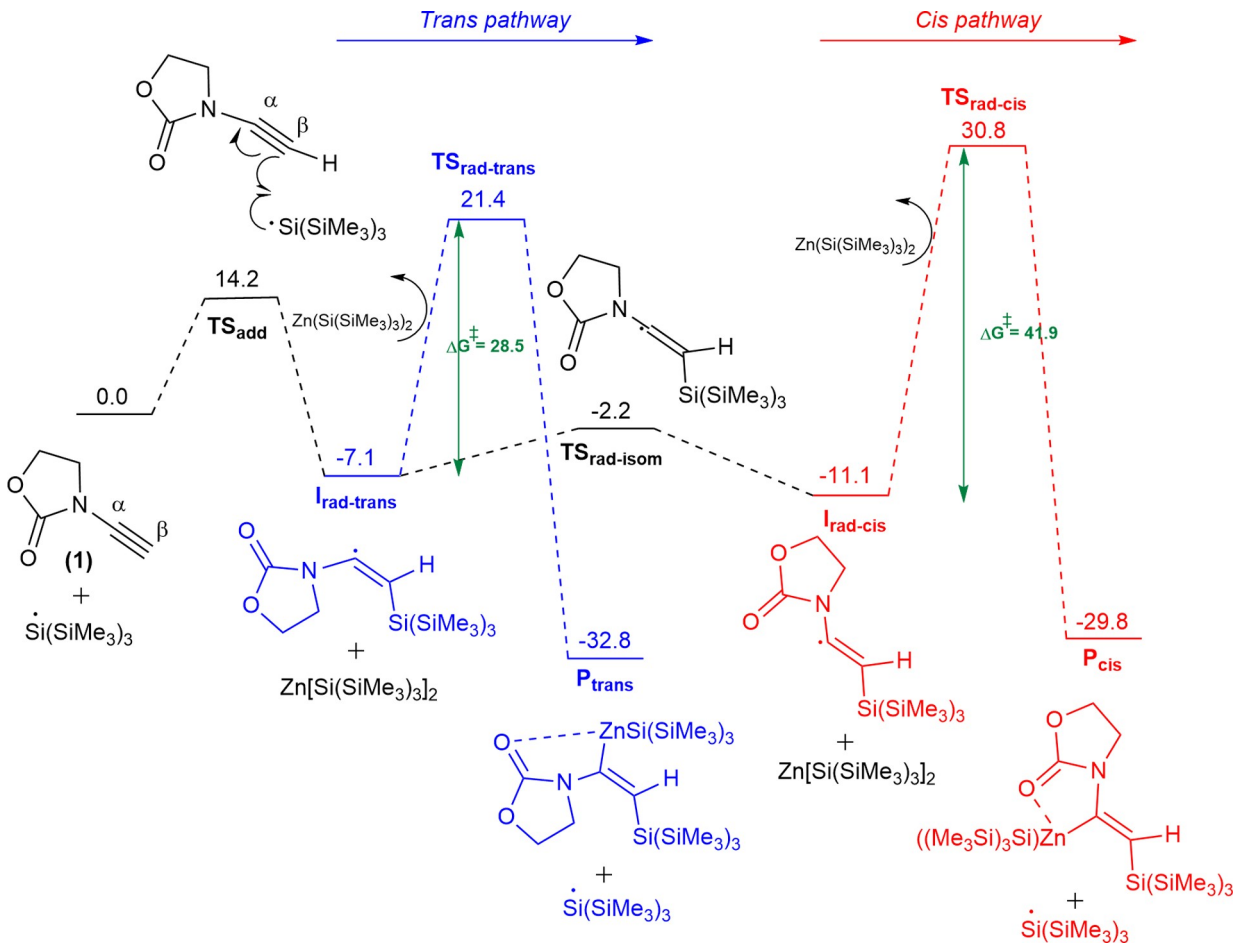

Figure 1. Gibbs energy profiles (in kcal mol^{-1}) for the radical *cis*- (red) and *trans*- (blue) silylzincation of ynamide **1** by $[(Me_3Si)_3Si]_2Zn$ (with respect to separated reactants, **1** and $(Me_3Si)_3Si$ radical).

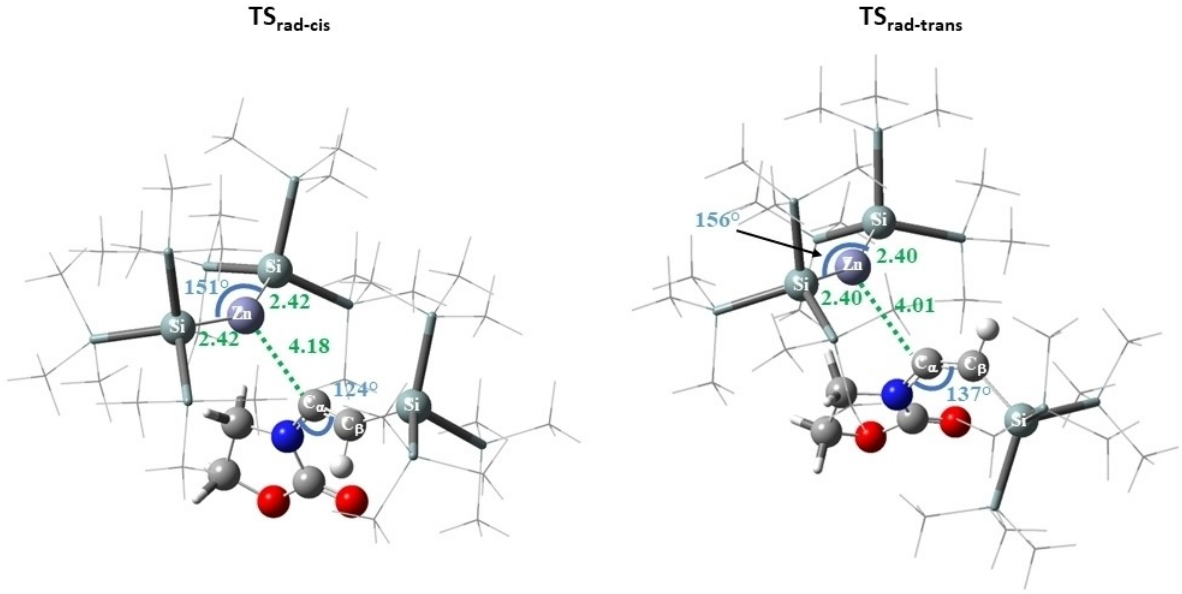

Figure 2. Structures of the radical transition states $TS_{rad-cis}$ (left, *cis*-silylzincation, 41.9 kcal mol^{-1} Gibbs energy barrier) and $TS_{rad-trans}$ (right, *trans*-silylzincation, 28.5 kcal mol^{-1} Gibbs energy barrier). Angles are given in degrees, distances in Å.; most methyl groups are omitted for clarity.

distances of 4.18 and 4.01 Å for $\mathbf{TS}_{\mathbf{rad\text{-}cis}}$ and $\mathbf{TS}_{\mathbf{rad\text{-}trans}}$, respectively. The Zn–$C_\alpha$ bonds are thus very far to be formed as they are more than 2 Å larger than in the products (2.01 and 1.99 Å in $\mathbf{P}_{\mathbf{cis}}$ and $\mathbf{P}_{\mathbf{trans}}$). This is corroborated with the slightly elongated Zn–Si bond in the two TS (2.42 and 2.40 Å in $\mathbf{TS}_{\mathbf{rad\text{-}cis}}$ and $\mathbf{TS}_{\mathbf{rad\text{-}trans}}$ *vs.* 2.34 Å in free $[(Me_3Si)_3Si]_2Zn$) which indicated the beginning of the $(Me_3Si)_3Si$ radical release. In addition, the bending of $(Me_3Si)_3Si]_2Zn$ is noticeably comparable between $\mathbf{TS}_{\mathbf{rad\text{-}cis}}$ and $\mathbf{TS}_{\mathbf{rad\text{-}trans}}$ (Si–Zn–Si angle of 151 and 156°, respectively *vs.* 180° in free $[(Me_3Si)_3Si]_2Zn$). A slight difference is noted for the N–C_α–C_β angle, which is more constrained for *cis* **TS** with an angle of 124° compared to 137° for the *trans* one, close to 138° in $\mathbf{I}_{\mathbf{rad\text{-}trans}}$ or $\mathbf{I}_{\mathbf{rad\text{-}cis}}$. The preference for the *trans* pathway by almost 10 kcal mol^{-1}is attributed to the large distortion energy for *cis* pathway (19 *vs.* 9.6 kcal mol^{-1} for *cis* and *trans*-pathway, respectively, Table S2), following the *activation strain* model.[25–27]

The polar mechanisms are next investigated inspired by previous studies.[21,22] The *cis*-product is first formed by the well-known *cis*-silylmetalation[5,28,29] and the *trans*-product is obtained through an isomerization step occurring *via* a metallocyclopropene intermediate The formation of the *cis*-product $\mathbf{P}_{\mathbf{cis}}$ (in red in Figure 3, geometrical parameters are given in Table S3) is highly exergonic (−29.8 kcal mol^{-1}) and thus irreversible. It is associated with a high activation barrier of 32.6 kcal mol^{-1}, nevertheless lower than that computed for the *cis* radical mechanism (41.9 kcal mol^{-1}, see Figure 1). This is in good agreement with the introductory statement that *cis*-addition is related to a polar mechanism. The *cis* transition state $\mathbf{TS}_{\mathbf{polar\text{-}cis}}$ involves a suprafacial process[30] wherein the Si–C_β and Zn–C_α σ bonds are formed on the same side of the reacting π-system as evidenced in Figure 4, by a quasi-planar dihedral angle of 32° between Zn–Si and C_α–C_β fragments.

The formation of the *trans*-product is envisioned *via* the isomerization step of the *cis*-product through $\mathbf{TS}_{\mathbf{polar\text{-}isom}}$ computed at 22.9 kcal mol^{-1} relative to the separated reactants. This TS (Figure 4) is associated with the H_β rotation from *cis* to *trans* to the zinc moiety, indicated by the orthogonal H_β position out of Zn–C_α–C_β plane (dihedral angle of 101° between Zn–C_α and C_β–H_β bonds). The shorter Zn–C_β bond of 2.03 Å and Zn–C_α bond of 2.10 Å, as well as the longer C_α–C_β distance of 1.47 Å, intermediate between a double and simple bond, are character-

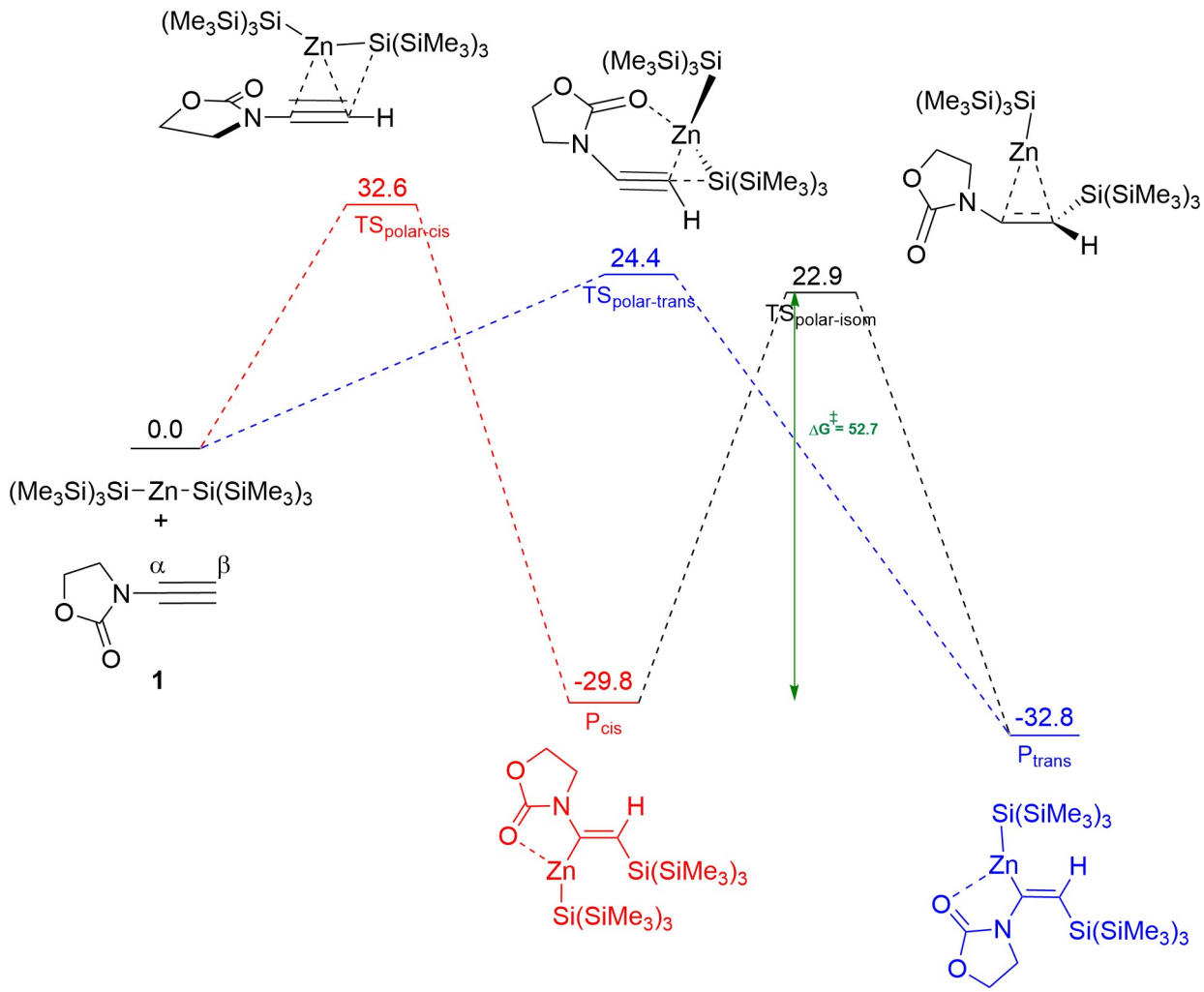

Figure 3. Gibbs energy profiles (in kcal mol^{-1}) for the polar *cis*- (red) and *trans*- (blue) silylzincation of ynamide **1** by $[(Me_3Si)_3Si]_2Zn$ (with respect to separated reactants, **1** and $[(Me_3Si)_3Si]_2Zn$).

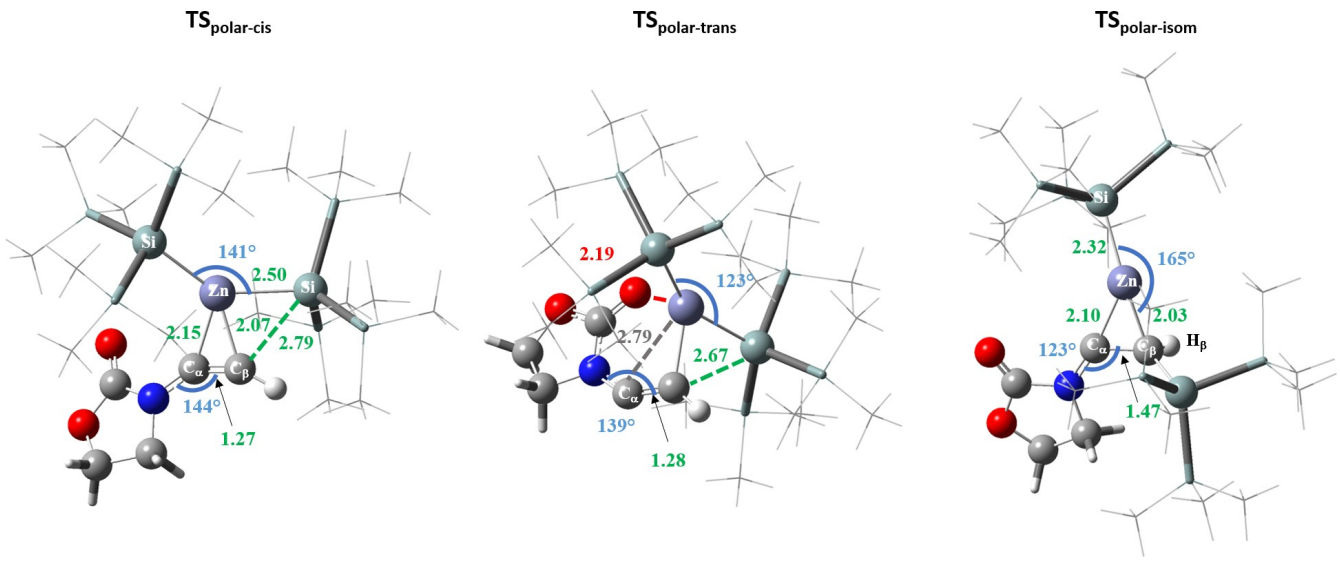

Figure 4. Structures of the polar transition states $\mathbf{TS}_{\text{polar-cis}}$ (left, *cis*-silylzincation, 32.6 kcal mol^{-1} Gibbs energy barrier), $\mathbf{TS}_{\text{polar-trans}}$ (center, *trans*-silylzincation, 24.4 kcal mol^{-1} Gibbs energy barrier) and $\mathbf{TS}_{\text{polar-isom}}$ (right, isomerization from *cis*- to *trans*-products, 52.7 kcal mol^{-1} Gibbs energy barrier). Angles are given in degrees, distances in Å.; most methyl groups are omitted for clarity.

istic of metallocyclopropene intermediate.[31] Indeed, this structure is similar to the structure reported by Trost and co-workers,[21] optimized as a minimum, for hydrosilylation of terminal alkynes by cationic ruthenium catalysts. Our attempt to locate a metallocyclopropene intermediate as a local minimum was not successful probably due to low ability of zinc(II) metal to react as a π-back-bonders. As a conclusion, the formation of *trans*-product $\mathbf{P}_{\text{trans}}$ from isomerization of *cis*-product $\mathbf{P}_{\text{cis}}$ through this peculiar $\mathbf{TS}_{\text{polar-isom}}$ is not kinetically accessible considering the high activation barrier (52.7 kcal mol^{-1} between $\mathbf{P}_{\text{cis}}$ and $\mathbf{TS}_{\text{polar-isom}}$ *vs.* 28.5 kcal mol^{-1} for *trans* radical pathway, see Figure 1).

To our surprise, we also located a transition state leading directly to the *trans*-product in only one step from reactants (in blue in Figure 3, geometries are given in Figure 4 and Table S2). This transition state $\mathbf{TS}_{\text{polar-trans}}$ is associated with an antarafacial process[30,32] where Si–C_β and Zn–C_α bonds are formed from opposite sides of the π-system as indicated by the Zn–Si bond twisted over the C_α–C_β bond (C_β–C_α–Zn–Si = 46°). This transition state also appears slightly more product-like than the *cis* one, with shorter Si–C_β (2.67 in $\mathbf{TS}_{\text{polar-trans}}$ *vs.* 2.79 Å in $\mathbf{TS}_{\text{polar-cis}}$) despite similar Zn–Si bonds (2.51 *vs.* 2.50 Å). More interesting, this antarafacial mechanism is an asynchronous process as the major geometrical change around the transition state is associated with the Si-C_β bond formation (Figure S2). The Zn–C_α is formed during large geometrical rearrangement described by a relaxation to reach the trans-product. The activation barrier of this concerted mechanism is computed at 24.4 kcal mol^{-1}, lower than that calculated for the radical pathway (28.5 kcal mol^{-1} between $\mathbf{I}_{\text{rad-trans}}$ and $\mathbf{TS}_{\text{rad-trans}}$, see Figure 1). As the energies of polar and radical species are possibly sensitive to the methodology used, the *trans*-activation barrier was calculated for polar and radical chain mechanism for various DFT functionals and basis sets as described in the Computational Details. This test confirms the lowest barrier for concerted mechanism over the radical pathway. Hence this computational finding suggests that the *trans*-silylzincation of terminal ynamides by reaction with $[(Me_3Si)_3Si]_2Zn$ proceeds through a concerted polar mechanism rather than a radical chain one. The consistency of the experimental observations regarding stereo- and regioselectivity with this new mechanism is then investigated.

As reminder, the stereoselectivity of the silylzincation of terminal ynamides is dependent on the silyl group of the silylzinc reagent: $(Me_2PhSi)_2Zn$ gives the *cis* whereas $[(Me_3Si)_3Si]_2Zn$ gives the *trans* product. The competition between the proposed supra- and antarafacial pathways is thus explored for $(Me_2PhSi)_2Zn$ (Table 1, Table S4 and Figure S3-S4) and $[(Me_3Si)_3Si]_2Zn$ (Figure 3, Table 1). For $(Me_2PhSi)_2Zn$, the highly exergonic reaction (−56.1 and −50.8 kcal mol^{-1}, respectively for *cis* and *trans* products, noted $\mathbf{P}_{\text{C-cis}}$ and $\mathbf{P}_{\text{C-trans}}$) is thermodynamically and kinetically favored for the *cis* pathway with a very small *cis* activation barrier (8.6 *vs.* 9.9 kcal mol^{-1} for $\mathbf{TS}_{\text{C-Cis}}$ and $\mathbf{TS}_{\text{C-trans}}$, respectively).[33] As previously discussed, a reverse selectivity is computed for $[(Me_3Si)_3Si]_2Zn$ in favor of the *trans* product (−32.8 kcal mol^{-1} *vs.* −29.8 kcal mol^{-1} for $\mathbf{P}_{\text{polar-trans}}$ and $\mathbf{P}_{\text{polar-cis}}$, respectively and 24.4 *vs.* 32.6 kcal mol^{-1} for $\mathbf{TS}_{\text{polar-}}$

Table 1. Gibbs energy for the transition states (TS) and products (P) (in kcal mol^{-1}, with respect to the separated reactants) for the concerted mechanism.

Regioselectivity	Si_2Zn	*cis*		*trans*	
		TS	P	TS	P
C_β	$[(Me_3Si)_3Si]_2Zn$	32.6	−29.8	**24.4**	**−32.8**
	$(Me_2PhSi)_2Zn$	**8.6**	**−56.1**	9.9	−50.8
C_α	$[(Me_3Si)_3Si]_2Zn$	40.9	−15.6	33.7	−28.0
	$(Me_2PhSi)_2Zn$	10.2	−43.3	14.5	-48.0

$_{trans}$ and $\mathbf{TS}_{polar\text{-}cis}$, respectively). The proposed polar mechanism is thus in line with experimentally observed stereoselectivity dependence on the silyl group.

The experimental observed regioselectivity in favor of the β-isomer (C_β–Si bond formed) is next examined. The results for the α-addition of $[(Me_3Si)_3Si]_2Zn$ or $(Me_2PhSi)_2Zn$ with **1** are given in Table 1 (Tables S5-S6 and Figures S5-S6). For the observed *trans*-mechanism, the β-addition is kinetically and thermodynamically favored by 9.3 (between $\mathbf{TS}_{polar\text{-}trans}$ and $\mathbf{TS}_{\alpha\text{-}trans}$) and 4.8 kcal mol^{-1} (between $\mathbf{P}_{polar\text{-}trans}$ and $\mathbf{P}_{\alpha\text{-}trans}$), respectively, over the α-addition (the results for the *cis*-addition are 8.3 and 14.6 kcal mol^{-1}, respectively). The computed regioselectivity for the concerted mechanisms is in accordance with the experimental results, independently of the silyl group used. Hence, the retained mechanism leading either to the *cis*- or *trans*-products in only one step successfully reproduces also the experimental regioselectivity.

To understand the difference of stereo- and regioselectivity, we have performed the decomposition of the activation energy $\Delta\Delta E^{\neq}$ into distortion ($\otimes\Delta E^{\neq}_{distortion}$) and interaction ($\otimes\Delta E^{\neq}_{interaction}$) energies following the fragment-based approach named *activation strain* model (Figure S7).[25–27] The results of this activation strain analysis are given in Table 2 for all transition states. In addition, we have performed this analysis along reaction coordinates (Si–C_β, Zn–C_α and C_α–C_β) in the transition state (Figures S8-S10).[26] For the $[(Me_3Si)_3Si]_2Zn$ species, the larger activation energy of 12.7 kcal mol^{-1} obtained for $\mathbf{TS}_{polar\text{-}cis}$ is essentially due to the distortion energy (38.0 and 32.1 kcal mol^{-1} for $\mathbf{TS}_{polar\text{-}cis}$ and $\mathbf{TS}_{polar\text{-}trans}$, respectively, see Table 2), as the interaction energies are quite similar (−25.3 and −27.7 kcal mol^{-1} for $\mathbf{TS}_{polar\text{-}cis}$ and $\mathbf{TS}_{polar\text{-}trans}$, respectively). This observation remains valid all along the reaction coordinate (Figure S9a). For a smaller substituent, like $SiMe_2Ph$, which should induce less steric hindrance, the distortion and interaction energies are very different than $[(Me_3Si)_3Si]_2Zn$: for the *cis*-addition, the high interaction energy (−49.0 kcal mol^{-1} for $\mathbf{TS}_{C\text{-}cis}$) is compensated by high strain energy (41.1 kcal mol^{-1} for $\mathbf{TS}_{C\text{-}cis}$) leading to a small activation barrier. This is confirmed all along the reaction path (Figure S9c). We can thus propose that the *cis*-pathway for $[(Me_3Si)_3Si]_2Zn$ is disfavoured because of steric hindrance of $(Me_3Si)_3Si$, which forces ynamide to undergo a larger distortion in order to welcome the addition of the disylilzinc reagent on the same side of the π system.

The distortion interaction analysis was also performed for $[(Me_3Si)_3Si]_2Zn$ to understand the regioselectivity in favor of β-addition. As already described for this species, the dominant contribution to the selectivity (difference in $\otimes\Delta E^{\neq}$) is the distortion energy. For the (preferred) *trans*-pathway, it is more than 10 kcal mol^{-1} higher for α-addition (44.1 kcal mol^{-1} for $\mathbf{TS}_{\alpha\text{-}trans}$, Table 2) over β-addition (32.1 kcal mol^{-1} for $\mathbf{TS}_{polar\text{-}trans}$), in contrast to a difference smaller than 3 kcal mol^{-1} in interaction energy. This higher $\otimes\Delta E^{\neq}_{distortion}$ is principally caused by the distortion energy of ynamide, higher for $\mathbf{TS}_{\alpha\text{-}trans}$ (29.6 kcal mol^{-1} *vs.* 21.3 kcal mol^{-1} for $\mathbf{TS}_{polar\text{-}trans}$, see Figure S10). We propose thus that the $(Me_3Si)_3Si$ addition into C_α in ynamide is disfavored because of the steric hindrance at C_α substituted by oxazolidinone group.

This regioselectivity in favor of β-addition of diorganosilylzinc reagents on C≡C triple bond of terminal alkyne can be considered as a reverse polarity process considering the polarization of ynamide. Indeed, the electron donating ability of the nitrogen atom of oxazolidinone group enables the ketenimininium resonance structure of ynamides, rendering C_α as the electrophilic site and C_β as the nucleophilic center. This is in accordance with the atomic charges calculated in **1** (Figure 5, Table S7): as expected, the charges on C_α and C_β are 0.15 and −0.27e, respectively, corresponding well to a nucleophilic site on C_β under charge control.[34] In $[(Me_3Si)_3Si]_2Zn$, the Zn–Si bond is polarized and the corresponding charge on Zn and Si are calculated at 1.16 and −0.89 (Figure 5, Table S7). From the point of view of charges, the silyl addition on ynamide occurs between two nucleophilic partners. The polar mechanism is generally associated with zwitterionic or ion-pair intermediates. In the present case, the polar term used in our previous studies to contrast with the radical mechanism, is not appropriate considering the low polarization of the C≡C bond during the

Table 2. Activation, Interaction and Distortion Energies (in kcal mol^{-1}) for $\mathbf{TS}_{polar\text{-}cis}$, $\mathbf{TS}_{polar\text{-}trans}$, $\mathbf{TS}_{C\text{-}cis}$, $\mathbf{TS}_{C\text{-}trans}$, $\mathbf{TS}_{\alpha\text{-}cis}$ and $\mathbf{TS}_{\alpha\text{-}trans}$ transition states using the *activation strain* model. The distortion energy $\otimes\Delta E^{\neq}_{distortion}$ is decomposed into the distortion energies of the two fragments: diorganosilylzinc $\otimes\Delta E^{\neq}_{ZnSi2}$ and **1** ($\otimes\Delta^{\neq}E_1$).

	Activation	Interaction	Distortion		
	$\Delta E^{\neq}$	$\Delta E^{\neq}_{interaction}$	$\Delta E^{\neq}_{distortion}$	$\Delta E^{\neq}_{ZnSi2}$	$\Delta E_1{}^{\neq}$
$\mathbf{TS}_{polar\text{-}cis}$	12.7	−25.3	38.0	16.5	21.5
$\mathbf{TS}_{polar\text{-}trans}$	4.4	−27.7	32.1	10.8	21.3
$\mathbf{TS}_{C\text{-}cis}$	−7.9	−49.0	41.1	12.2	28.9
$\mathbf{TS}_{C\text{-}trans}$	−5.5	−28.8	23.3	5.5	17.8
$\mathbf{TS}_{\alpha\text{-}cis}$	21.0	−37.7	58.7	21.0	37.7
$\mathbf{TS}_{\alpha\text{-}trans}$	13.6	−30.5	44.1	14.6	29.6

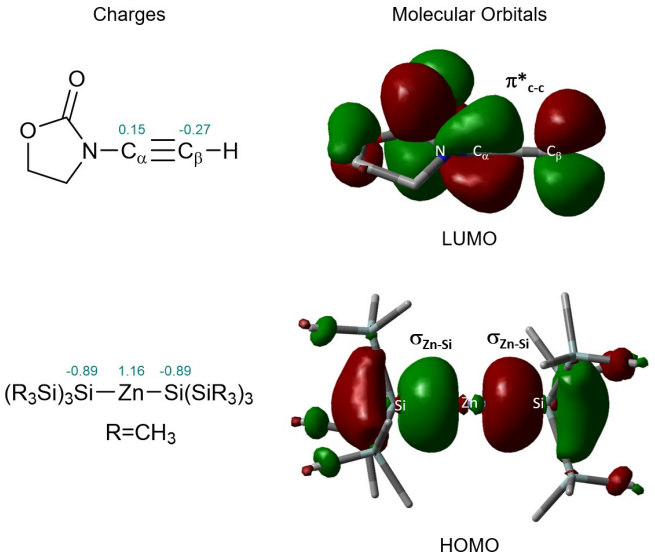

Figure 5. Atomic charges obtained through the Natural Population Analysis method and selected Molecular Orbitals (isovalue: 0.04 a.u., H are omitted for clarity) for **1** and $[(Me_3Si)_3Si]_2Zn$.

process (Table S7). The two proposed antara- (*trans*) and suprafacial (*cis*) additions are thus better viewed as "closed shell" concerted mechanisms. Taking account the HOMO molecular orbitals of $\mathbf{TS}_{\text{polar-trans}}$, given in Figure 6, the contribution of orbital fragments associated with the $\sigma_{Zn\text{-}Si}$ Zn–Si bond of $[(Me_3Si)_3Si]_2Zn$ (corresponding to its HOMO shown in Figure 5) and one of the $\pi^*_{C\text{-}C}$ $C_\alpha \equiv C_\beta$ bond (corresponding to its LUMO given in Figure 5) corresponds to a nucleophilic attack of silyl group to the electrophilic ynamide. This corroborates the Natural Bonding Orbital (NBO) analysis in the TS structure, in which a Lone Pair (LP) of the reactive silyl group interacts with the $\pi^*_{C\text{-}C}$ ynamide from a donor-acceptor interactions scheme ($E = 52{,}28$ kcal mol^{-1}).[35] The silyl addition is thus described, under an orbital control, as a nucleophilic attack of silyl group to the electrophilic ynamide

It is also known that the oxazolidinone group on ynamide can reverse the regioselectivity in favor of the β-addition through a metal-carbonyl chelation.[36] In our study, we find this secondary interaction between the Zn center and the oxygen atom of the carbonyl group from oxazolidinone[35–36] only for *trans*-additions, described by a short Zn–O distance of 2.19 Å in β-addition $\mathbf{TS}_{\text{polar-trans}}$ (Figure 4, Table S3) and 2.16 Å in α-addition $\mathbf{TS}_{\alpha\text{-trans}}$ (Table S5). As this Zn–O distance is present in the two regioselective TS, we can conclude that a Zn–Carbonyl chelation is not a factor that changes the regioselectivity of this reaction. We evaluate the Zn–O interaction energy at 8.5 kcal mol^{-1} (Figure S11, Table S8) by comparing the energies of the two *trans* transition states ($\mathbf{TS}_{\text{polar-trans}}$ *vs.* $\mathbf{TS}_{\text{polar-trans-conf}}$) in which the conformations of oxazolidinone group are different. In $\mathbf{TS}_{\text{polar-trans-conf}}$ the oxygen of carbonyl group is pointed at the opposite of the zinc moiety to avoid a Zn–O secondary interaction. The *trans* transition state without Zn–O interaction ($\mathbf{TS}_{\text{polar-trans-conf}}$) is computed at 32.9 kcal mol^{-1} and competes with the stereoselective *cis*-transition state (32.6 kcal mol^{-1} for $\mathbf{TS}_{\text{polar-cis}}$, see Figure S11). We can thus propose that this Zn–O interaction is not innocent as it strongly stabilizes $\mathbf{TS}_{\text{polar-trans}}$ (24.4 kcal mol^{-1}) over $\mathbf{TS}_{\text{polar-cis}}$ leading thus to a stereoselectivity in favor of the *trans*-product. This Zn–O interaction is not present for $\mathbf{TS}_{\text{polar-cis}}$ (3.90 Å) as the suprafacial process positioning the zinc center too far from the carbonyl function to be accessible. The Zn–O metal-carbonyl chelation can thus reverse the stereoselectivity of this reaction.

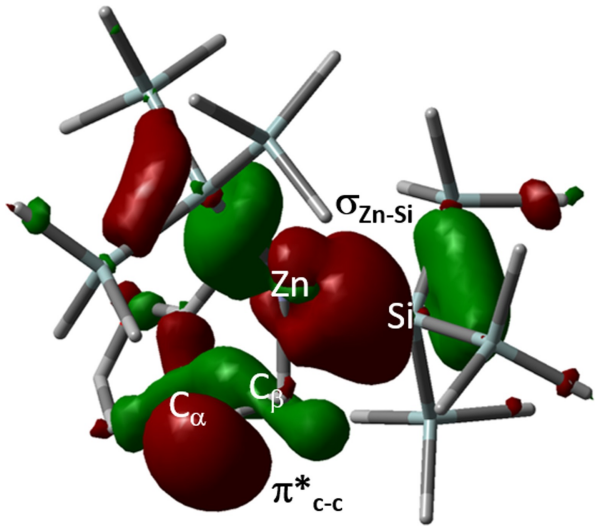

Figure 6. Highest Occupied Molecular Orbital of $\mathbf{TS}_{\text{polar-trans}}$ (isovalue: 0.03 a.u., H are omitted for clarity).

Conclusions

In conclusion, we show that the addition of diorganosilyl-zinc reagents across terminal ynamides can take place through a one-step concerted addition with a lower activation barrier than that of the originally proposed radical pathway[7] and that of a possible *cis* to *trans* isomerization process.[18,19,21,22] This concerted mechanism occurs either in a suprafacial or antarafacial manner, leading respectively to a *cis*- or *trans*-addition. The antarafacial mechanism resulting in the formation of a Si–C and a Zn–C σ-bond on opposite sides of the π-system is compatible with the observed regio- and stereo-selectivities. As revealed by the *activation strain* analysis, the *trans*-stereoselectivity for $[(Me_3Si)_3Si]_2Zn$ is partially due to the steric effect of the silyl group and is assisted by the oxazolidinone group. In the same way, the regioselectivity is explained by the bulkiness of ynamide carbon substituted by oxazolidinone group. Our new findings thus call for analyzing the effect of substituents in terminal alkyne and characterizing the bonding scheme of these concerted transition states along the reaction coordinate. Most importantly, beyond ynamide silylzincation chemistry, we believe that this new *trans*-concerted mechanism can be relevant to a large variety of addition mechanisms to carbon–carbon multiple bonds involving late transition metal complexes, either in replacement or in competition with the isomerization mechanisms proposed in the literature.[14–16,18–23]

Computational Details

The calculations are carried out with Gaussian16 package.[38] All geometries are calculated using the hybrid B3PW91[39] functional and the 6–31G(d,p) basis set[40] for all atoms. The geometry optimizations are performed without any constraint and the nature of the extrema are verified by analytical calculations of frequencies. The connection between TS and minima is confirmed by carrying out a small displacement along the reaction coordinate in each direction and optimizing geometry starting from these structures. Two reactant complexes are located for *cis* and *trans*-pathways with $(Me_2PhSi)_2Zn$ and $[(Me_3Si)_3Si]_2Zn$ and are not added in the Gibbs Energy profile, as they do not change the activation barrier for *cis*- and *trans*-additions. Their structures and energies are given in Figure S12. The Gibbs free energies are calculated assuming an ideal gas, unscaled harmonic frequencies, and the rigid rotor approximation in the standard conditions ($P = 1$ atm and $T = 298$ K). Density-based Solvation Model (SMD)[41] single point calculations are performed using experimental solvents: n-hexane for $[(Me_3Si)_3Si]_2Zn$ and diethylether for $(Me_3Si)_2Zn$. The results of these single points calculations are given in the Supporting Information (Tables S9 and S10) and confirm that the *trans*-addition is favored over the *cis*-one. To investigate the competition of polar and radical chain mechanisms, a series of functionals and basis sets, detailed in

Table 3. Gibbs energies of activation barrier (in kcal mol^{-1}) for *trans*-silylzincation of $[(Me_3Si)_3Si]_2Zn$ in ynamide **1** in polar (Figure 3, relative to separated reactants) and radical chain mechanisms (Figure 1, with respect to $I_{rad\text{-}trans}$) using a series of DFT functional and basis set.

DFT functional/basis set	$\Delta G^{\ddagger}(TS_{polar\text{-}trans})$	$\Delta G^{\ddagger}(TS_{rad\text{-}trans})$
B3PW91 6–31G(d,p)	24.4	28.5
PW91 6–31G(d,p)	10.4	19.3
CAM B3LYP 6–31G(d,p)	23.8	23.6
B3PW91 def2svp	30.5	30.8
B3PW91 6–31G(d,p), SDD ECP for Zn	31.2	32.5
B3PW91 6–311G(d,p)	32.3	33.0

Supporting Information, are used and the results are summarized in Table 3 (Tables S11–S13 for more details). The *trans* activation barrier of polar pathway is lower than that calculated for radical pathway, except for CAM–B3LYP functional. For this last one, the energy of radical *trans*-addition is more favorable by only 0.2 kcal mol^{-1} than the polar pathway. Considering this low energetic difference which is in the range of error of DFT calculations, we are confident in our results. The Natural Population Analysis (NPA) is used to evaluate the atomic charges[42] using the NBO package[43] available in Gaussian16.

Supporting Information

Additional computational data, cartesian coordinates of all intermediates and transition states and additional references [44–49] are provided in the Supporting Information.

Acknowledgements

This work was supported by LabEx MiChem of French state funds managed by the ANR within the Investissements d'Avenir programme under reference ANR-11-IDEX-0004-02.

Conflict of Interests

The authors declare no conflict of interest.

Data Availability Statement

The data that support the findings of this study are available in the supplementary material of this article.

Keywords: *trans*-concerted addition · silylzincation · radical · antarafacial · DFT

[1] D. S. W. Lim, E. A. Anderson, *Synthesis* **2012**, *44*, 983–1010.
[2] a) I. Fleming, T. W. Newton, F. Roessler, *J. Chem. Soc. Perkin Trans. 1* **1981**, 2527–2532; b) J. Hibino, S. Nakatsukasa, K. Fugami, S. Matsubara, K. Oshima, H. Nozaki, *J. Am. Chem. Soc.* **1985**, *107*, 6416–6417; c) H. Hayami, M. Sato, S. Kanemoto, Y. Morizawa, K. Oshima, H. Nozaki, *J. Am. Chem. Soc.* **1983**, *105*, 4491–4492; d) K. Wakamatsu, T. Nonaka, Y. Okuda, W. Tückmantel, K. Oshima, K. Utimoto, H. Nozaki, *Tetrahedron* **1986**, *42*, 4427–4436; e) Y. Okuda, K. Wakamatsu, W. Tűckmantel, K. Oshima, H. Nozaki, *Tetrahedron Lett.* **1985**, *26*, 4629–4632; f) G. Auer, M. Oestreich, *Chem. Commun.* **2006**, 311–313; g) Y. Okuda, Y. Morizawa, K. Oshima, H. Nozaki, *Tetrahedron Lett.* **1984**, *25*, 2483–2486; h) V. Liepins, A. S. E. Karlström, J.-E. Bäckvall, *J. Org. Chem.* **2002**, *67*, 2136–2143; i) J. Tang, H. Shinokubo, K. Oshima, K. Bull, *Chem. Soc. Jpn.* **1997**, *70*, 245–251.
[3] S. Nakamura, M. Uchiyama, T. Ohwada, *J. Am. Chem. Soc.* **2004**, *126*, 11146–11147.
[4] V. N. Bochatay, Z. Neouchy, F. Chemla, F. Ferreira, O. Jackowski, A. Pérez-Luna, *Synthesis* **2016**, *48*, 3287–3300.
[5] Y. Nagashima, D. Yukimori, C. Wang, M. Uchiyama, *Angew. Chem. Int. Ed.* **2018**, *57*, 8053–8057.
[6] E. Romain, C. Fopp, F. Chemla, F. Ferreira, O. Jackowski, M. Oestreich, A. Perez-Luna, *Angew. Chem. Int. Ed.* **2014**, *53*, 11333–11337.
[7] C. Fopp, E. Romain, K. Isaac, F. Chemla, F. Ferreira, O. Jackowski, M. Oestreich, A. Perez-Luna, *Org. Lett.* **2016**, *18*, 2054–2057.
[8] C. Fopp, K. Isaac, E. Romain, F. Chemla, F. Ferreira, O. Jackowski, M. Oestreich, A. Perez-Luna, *Synthesis* **2017**, *49*, 724–735.
[9] C. Chatgilialoglu, *Chem. Eur. J.* **2008**, *14*, 2310–2320.
[10] a) S. Bazin, L. Feray, M. P. Bertrand, *Chimia* **2006**, *60*, 260–265; b) J. Maury, L. Feray, M. Bertrand, *Org. Lett.* **2011**, *13*, 1884–1887; c) T. Akindele, K.-I. Yamada, K. Tomioka, *Acc. Chem. Res.* **2009**, *42*, 345–355.
[11] J. Maury, L. Feray, S. Bazin, J.-L. Clément, S. R. A. Marque, D. Siri, M. P. Bertrand, *Chem. Eur. J.* **2011**, *17*, 1586–1595.
[12] E. Romain, K. de la Vega-Hernández, F. Guégan, J. S. García, C. Fopp, F. Chemla, F. Ferreira, H. Gerard, O. Jackowski, S. Halbert, M. Oestreich, A. Perez-Luna, *Adv. Synth. Catal.* **2021**, *363*, 2634–2647.
[13] M. Yonehara, S. Nakamura, A. Muranaka, M. Uchiyama, *Chem. Asian J.* **2010**, *5*, 452–455.
[14] a) B. M. Bode, P. N. Day, M. S. Gordon, *J. Am. Chem. Soc.* **1998**, *120*, 1552–1555; b) S. Sakaki, M. Sumimoto, M. Fukuhara, M. Sugimoto, H. Fujimoto, S. Matsuzaki, *Organometallics* **2002**, *21*, 3788–3802; c) S. Sakaki, N. Mizoe, M. Sugimoto, *Organometallics* **1998**, *17*, 2510–2523.
[15] a) J. F. Harrod, A. J. Chalk, *J. Am. Chem. Soc.* **1964**, *86*, 1776–1779; b) A. J. Chalk, J. F. Harrod, *J. Am. Chem. Soc.* **1965**, *87*, 16–21.
[16] a) M. A. Schroeder, M. S. Wrighton, *J. Organomet. Chem.* **1977**, *128*, 345–358; b) C. L. Randolph, M. S. Wrighton, *J. Am. Chem. Soc.* **1986**, *108*, 3366–3374; c) A. Millan, E. Towns, P. M. Maitlis, *J. Chem. Soc. Chem. Commun.* **1981**, 673–674.
[17] A. Wooten, P. J. Carroll, A. G. Maestri, P. J. Walsh, *J. Am. Chem. Soc.* **2006**, *128*, 4624–4631.
[18] R. S. Tanke, R. H. Crabtree, *J. Am. Chem. Soc.* **1990**, *112*, 7984–7989.
[19] I. Ojima, N. Clos, R. J. Donovan, P. Ingallina, *Organometallics* **1990**, *9*, 3127–3133.
[20] C. H. Jun, R. H. Crabtree, *J. Organomet. Chem.* **1993**, *447*, 177–187.
[21] a) B. M. Trost, Z. T. Ball, *J. Am. Chem. Soc.* **2003**, *125*, 30–31; b) L. W. Chung, Y.-D. Wu, B. M. Trost, Z. T. Ball, *J. Am. Chem. Soc.* **2003**, *125*, 11578–11582.
[22] R. H. Crabtree, *New J. Chem.* **2003**, *27*, 771–772.
[23] R. Chandrasekaran, K. Selvam, T. Chinnusamy, T. Rajeshkumar, L. Maron, R. Rasappan, *Angew. Chem. Int. Ed. Accepted* e202318689.
[24] T.-D. Tan, Z.-S. Wang, P.-C. Qian, L.-W. Ye, *Small Methods* **2021**, *5*, 2000673–2000691.
[25] W.-J. van Zeist, F. M. Bickelhaupt, *Org. Biomol. Chem.* **2010**, *8*, 3118–3127.
[26] F. M. Bickelhaupt, K. N. Houk, *Angew. Chem. Int. Ed.* **2017**, *56*, 10070–10086.
[27] I. Fernández, F. M. Bickelhaupt, *Chem. Soc. Rev.* **2014**, *43*, 4953–4967.
[28] S. Mori, E. Nakamura, *J. Mol. Struct.* **1999**, *461–462*, 167–175.
[29] Y. Yamamoto, *J. Org. Chem.* **2018**, *83*, 12775–12783.
[30] a) F. A. Carey, R. J. Sundberg, In Advanced Organic Chemistry: Part A: Structure and Mechanisms; (Eds: F. A. Carey, R. J. Sundberg), Springer, Boston, **2007**, pp. 833–964; b) R. B. Woodward, R. Hoffmann, *Angew. Chem. Int. Ed. Engl.* **1969**, *8*, 781–853.
[31] D. S. Frohnapfel, J. L. Templeton, *Coord. Chem. Rev.* **2000**, *206–207*, 199–235.
[32] G. S. Hammond, *J. Am. Chem. Soc.* **1955**, *77*, 334–338.
[33] M. J. S. Dewar, *J. Am. Chem. Soc.* **1984**, *106*, 209–219.
[34] H. Lingua, F. Vibert, D. Mouysset, D. Siri, M. P. Bertrand, L. Feray, *Tetrahedron* **2017**, *73*, 3415–3422.
[35] To quantify the relationship between standard delocalized MOs and localized NBOs results, we employed the Canonical Molecular Orbital

Analysis (CMO), which gives the NBO description of each canonical molecular orbital. The major contributions in HOMO is from LP of Si (coefficient of -0.546) and the π^* of C-C (-0.29) in agreement with delocalized HOMO visualization.

[36] B. Zhou, T.-D. Tan, X.-Q. Zhu, M. Shang, L.-W. Ye, *ACS Catal.* **2019**, *9*, 6393–6406.

[37] M. Ito, R. Mitsuhashi, M. Mikuriya, H. Sakiyama, *X-Ray Struct. Anal. Online* **2016**, *32*, 21–22.

[38] Gaussian 16, Revision C.01, M. J. Frisch, G. W. Trucks, H. B. Schlegel, G. E. Scuseria, M. A. Robb, J. R. Cheeseman, G. Scalmani, V. Barone, G. A. Petersson, H. Nakatsuji, X. Li, M. Caricato, A. V. Marenich, J. Bloino, B. G. Janesko, R. Gomperts, B. Mennucci, H. P. Hratchian, J. V. Ortiz, A. F. Izmaylov, J. L. Sonnenberg, D. Williams-Young, F. Ding, F. Lipparini, F. Egidi, J. Goings, B. Peng, A. Petrone, T. Henderson, D. Ranasinghe, V. G. Zakrzewski, J. Gao, N. Rega, G. Zheng, W. Liang, M. Hada, M. Ehara, K. Toyota, R. Fukuda, J. Hasegawa, M. Ishida, T. Nakajima, Y. Honda, O. Kitao, H. Nakai, T. Vreven, K. Throssell, J. A. Montgomery, Jr., J. E. Peralta, F. Ogliaro, M. J. Bearpark, J. J. Heyd, E. N. Brothers, K. N. Kudin, V. N. Staroverov, T. A. Keith, R. Kobayashi, J. Normand, K. Raghavachari, A. P. Rendell, J. C. Burant, S. S. Iyengar, J. Tomasi, M. Cossi, J. M. Millam, M. Klene, C. Adamo, R. Cammi, J. W. Ochterski, R. L. Martin, K. Morokuma, O. Farkas, J. B. Foresman, and D. J. Fox, Gaussian, Inc., Wallingford CT, **2016**.

[39] a) J. P. Perdew, Y. Wang, *Phys. Rev. B* **1992**, *45*, 13244–13249; b) A. D. Becke, *J. Chem. Phys.* **1993**, *98*, 5648–5652.

[40] a) W. J. Hehre, R. Ditchfield, J. A. Pople, *J. Chem. Phys.* **1972**, *56*, 2257–2261; b) P. C. Hariharan, J. A. Pople, *Theor. Chim. Acta* **1973**, *28*, 213–222; c) M. Francl, W. J. Pietro, W. J. Hehre, J. S. Binkley, M. S. Gordon, D. J. DeFrees, J. A. Pople, *J. Chem. Phys.* **1982**, *77*, 3654–3665; d) V. A. Rassolov, J. A. Pople, M. A. Ratner, T. L. Windus, *J. Chem. Phys.* **1998**, *109*, 1223–1229.

[41] A. V. Marenich, C. J. Cramer, D. G. Truhlar, *J. Phys. Chem. B* **2009**, *113*, 6378–6396.

[42] A. E. Reed, L. A. Curtiss, F. Weinhold, *Chem. Rev.* **1988**, *88*, 899–926.

[43] NBO 6.0. E. D. Glendening, J. K. Badenhoop, A. E. Reed, J. E. Carpenter, J. A. Bohmann, C. M. Morales, C. R. Landis, and F. Weinhold (Theoretical Chemistry Institute, University of Wisconsin, Madison, WI, 2013), available in Gaussian16.

Manuscript received: May 3, 2024
Accepted manuscript online: May 29, 2024
Version of record online: July 11, 2024